Electronic Supplementary Material (ESI) for RSC Advances.

Supporting Information

Synthesis, Characterization, Electrochemical Properties and Catalytic Reactivity of the N-Heterocyclic Carbene-Containing Diiron Complexes

Yanhong Wang[1, 2], Tianyong Zhang[1, 2] *, Bin Li[1, 2]*, Shuang Jiang[1, 2], Liao Sheng[1, 2]

[1] School of Chemical Engineering and Technology, Tianjin Key Laboratory of Applied Catalysis Science and Technology, Tianjin University, Tianjin 300072, China.

[2] Collaborative Innovation Center of Chemical Science and Engineering (Tianjin), Tianjin 300072, China.

Table S1. Crystallographic data and refinement parameters for complexes **II** and **IV**.

Parameter	**II**	**IV**
Empirical formula	$C_{18}H_{22}Fe_2N_4O_4S_2$	$C_{30}H_{32}Fe_2N_2O_5S_2$
Formula weight	534.22	676.40
Temperature(K)	293(2)	113(2)
Wavelength(Å)	0.71073	0.71075
Crystal system	Orthorhombic	Orthorhombic
space group	Pbca	$Pna2_1$
a(Å)	13.733(3)	28.207(4)
b(Å)	14.889(3)	21.630(3)
c(Å)	21.978(4)	10.2634(12)
α(deg)	90	90
β(deg)	90	90
γ(deg)	90	90
Volume($Å^3$)	4494.1(16)	6261.7(13)
Z	8	8
Calculated density(mg/m^3)	1.579	1.435
Absorption coefficient(mm^{-1})	1.508	1.100
F(000)	2192	2800
Crystal size(mm)	0.20 x 0.18 x 0.12	0.24 x 0.18 x 0.16
Theta range for data collection(deg)	1.85 to 27.91	1.72 to 27.12
Limiting indices	-18≤h≤18 -19≤k≤19 -28≤l≤25	-36≤h≤36 -27≤k≤27 -12≤l≤13
Reflections collected	38038	69773
Reflections unique, R(int)	5364, 0.0462	13556, 0.0965
Completeness to theta =	27.91, 99.8%	27.12, 99.8%
Absorption correction	Semi-empirical from equivalents	Semi-empirical from equivalents
Max. and min. transmission	0.8397 and 0.7524	0.8436 and 0.7782
Data / restraints / parameters	5364 / 0 / 276	13556 / 73 / 798
Goodness-of-fit on F^2	1.079	1.077
Final R indices [I>2sigma(I)]	R1 = 0.0444 wR2 = 0.1115	R1 = 0.0668 wR2 = 0.1445
R indices (all data)	R1 = 0.0543 wR2 = 0.1187	R1 = 0.0847 wR2 = 0.1549
Largest diff. peak and hole(e A^{-3})	0.506 and -0.454	0.432 and -0.478

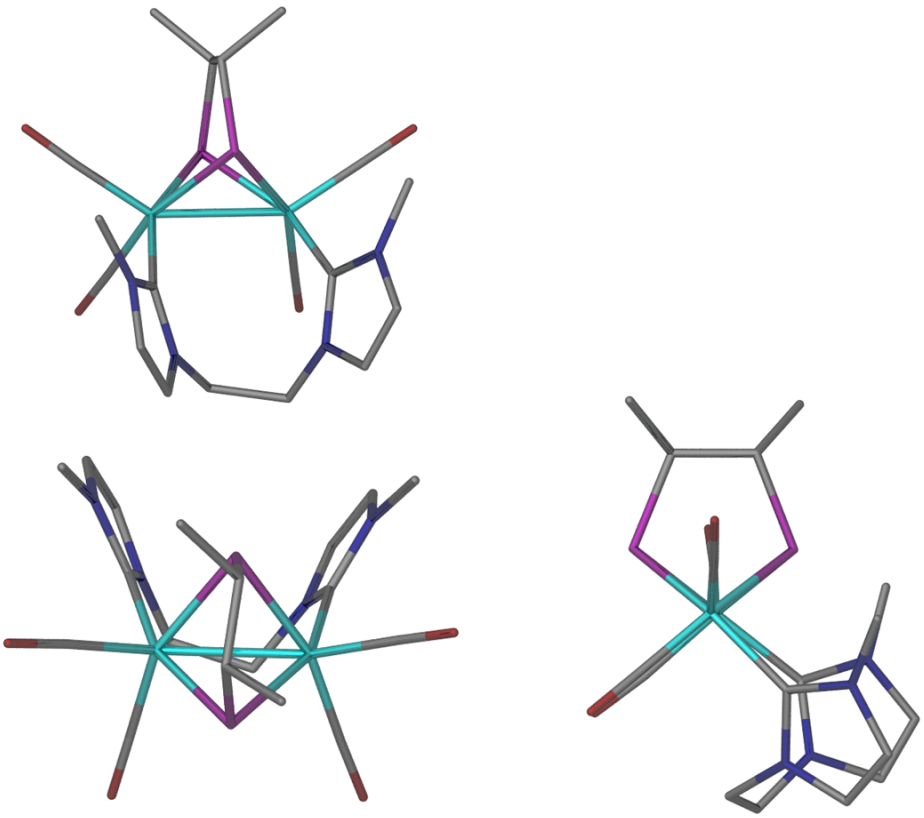

Figure S1. Stick drawing models of complex **II** given in three perspectives.

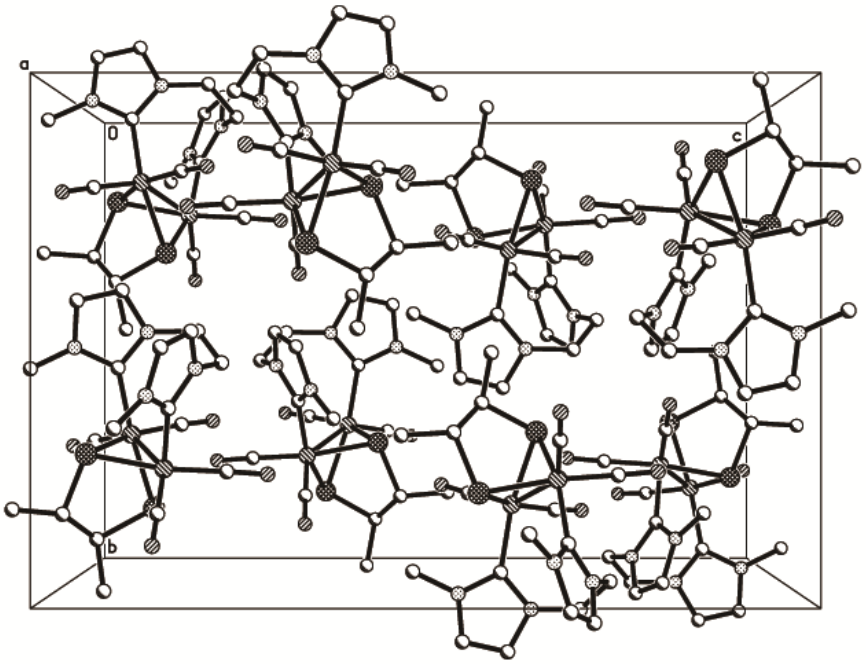

Figure S2. Unit cell of complex **II**.

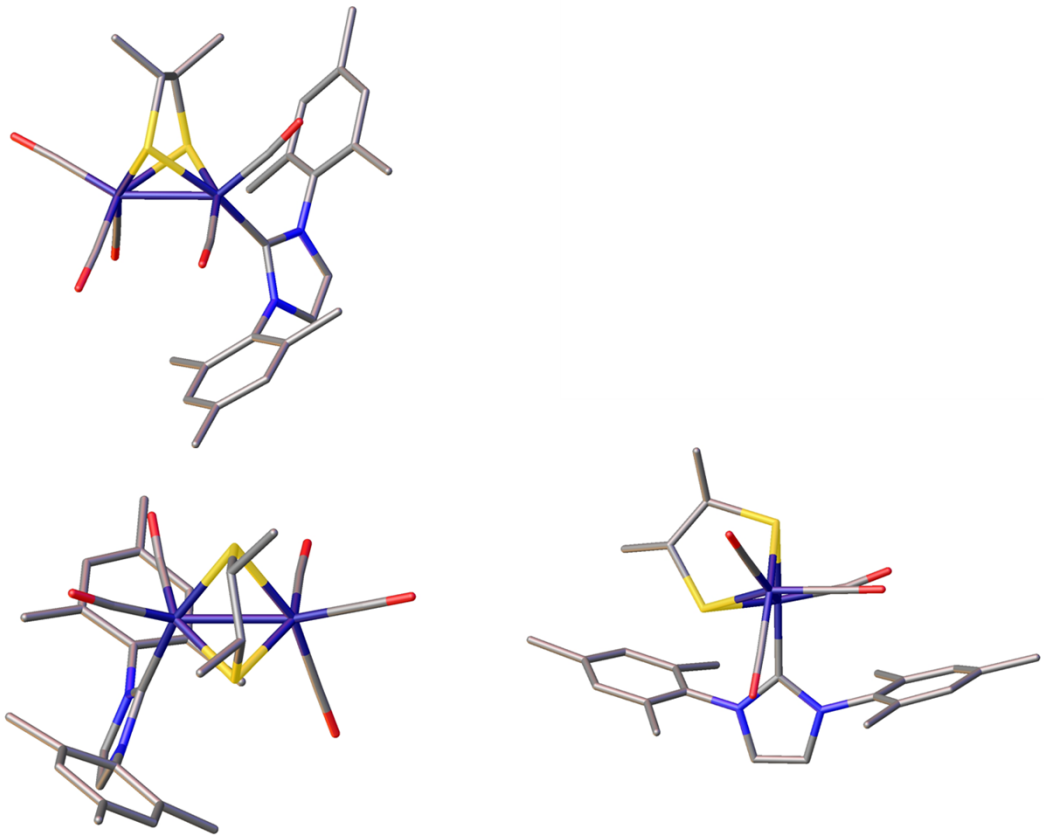

Figure S3. Stick drawing models of complex **IV** given in three perspectives.

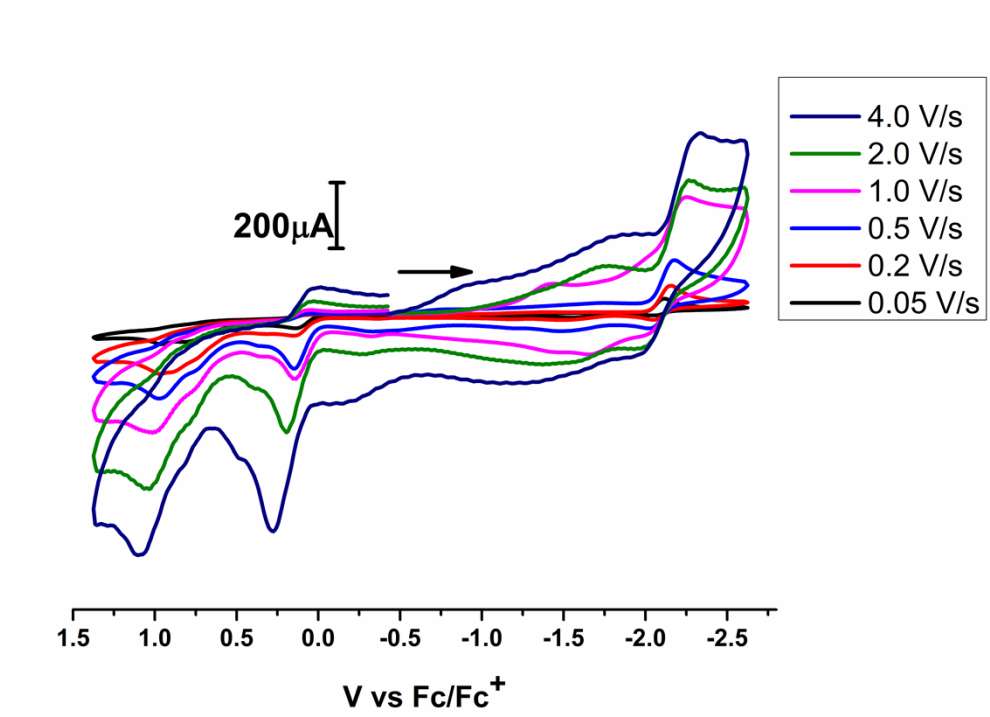

Figure S4. Cyclic voltammograms of the complex **IV** (2 mM) at various scan rates in CH_3CN solution (0.1 M *n*-Bu_4NPF_6) under N_2 at room temperature. All potentials are scaled to Fc/Fc^+=0.00 V.

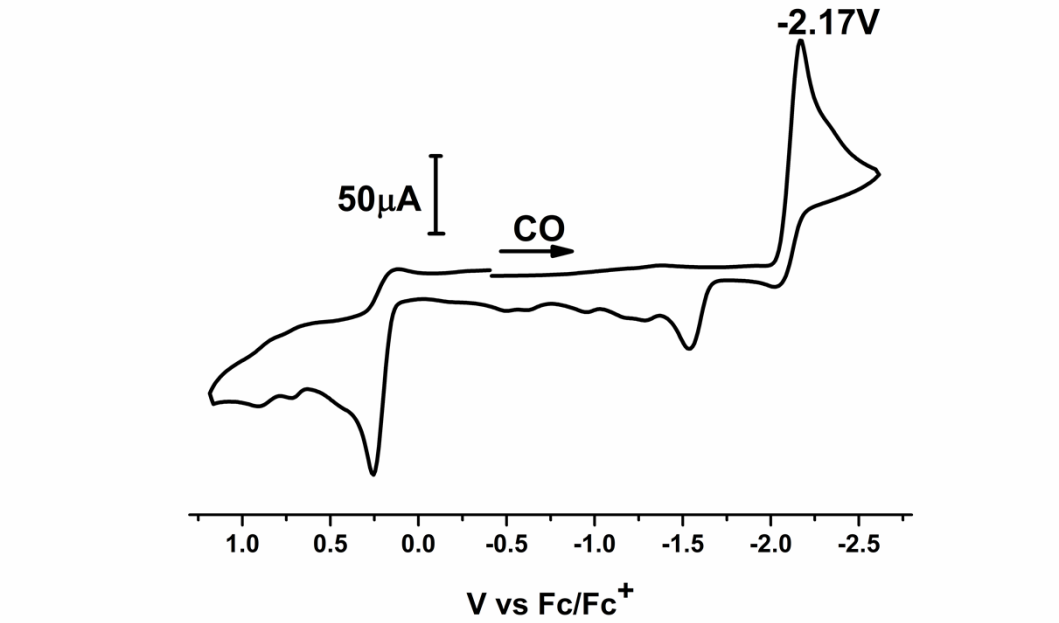

Figure S5. Cyclic voltammograms of the complex **V** (2 mM) in CH_3CN solution (0.1 M *n*-Bu_4NPF_6; scan rate, 200 mV/s) under CO at room temperature. All potentials are scaled to Fc/Fc^+=0.00 V.

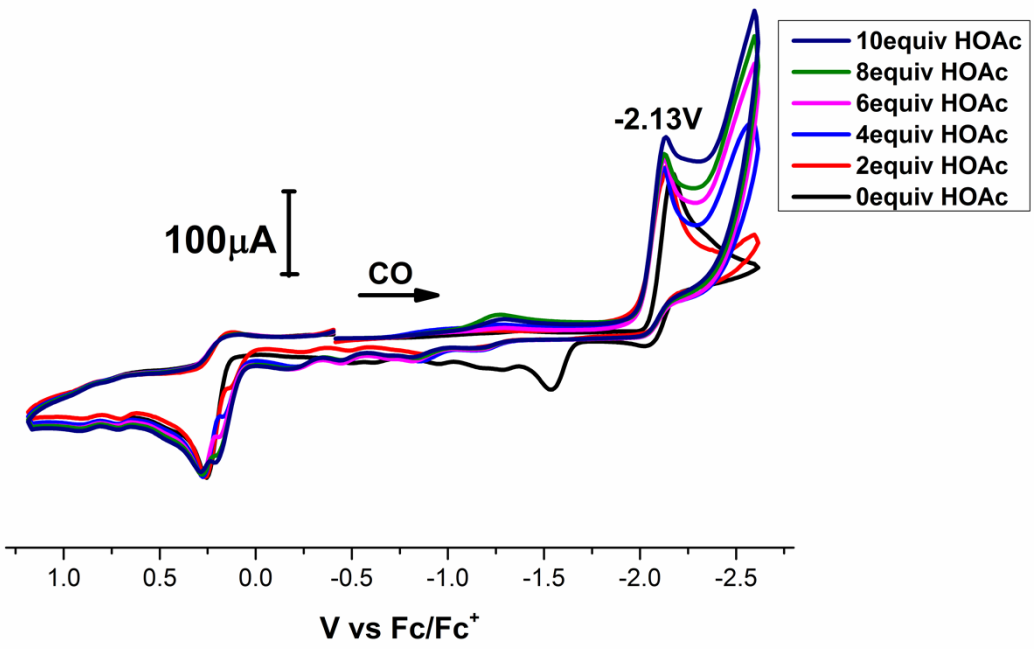

Figure S6. Cyclic voltammograms of the complex **V** (2 mM) with HOAc (0, 2, 4, 6, 8 and 10 equiv.) in CH_3CN solution (0.1 M *n*-Bu_4NPF_6; scan rate, 200 mV/s) under CO. All potentials are scaled to Fc/Fc^+=0.00 V.

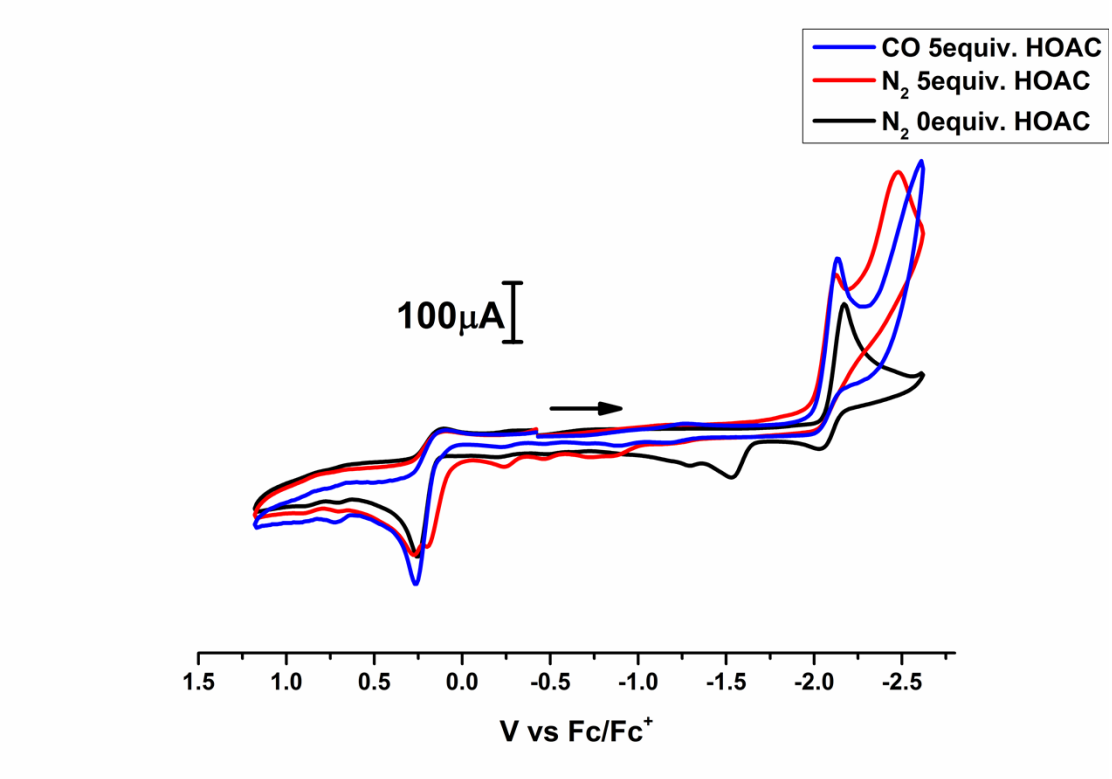

Figure S7. Cyclic voltammograms of the complex **V** (2 mM) in CH_3CN solution (0.1 M *n*-Bu_4NPF_6; scan rate, 200 mV/s) (black, under N_2) and with 5 equiv. HOAc (red, under N_2; blue under CO). All potentials are scaled to Fc/Fc^+=0.00 V.

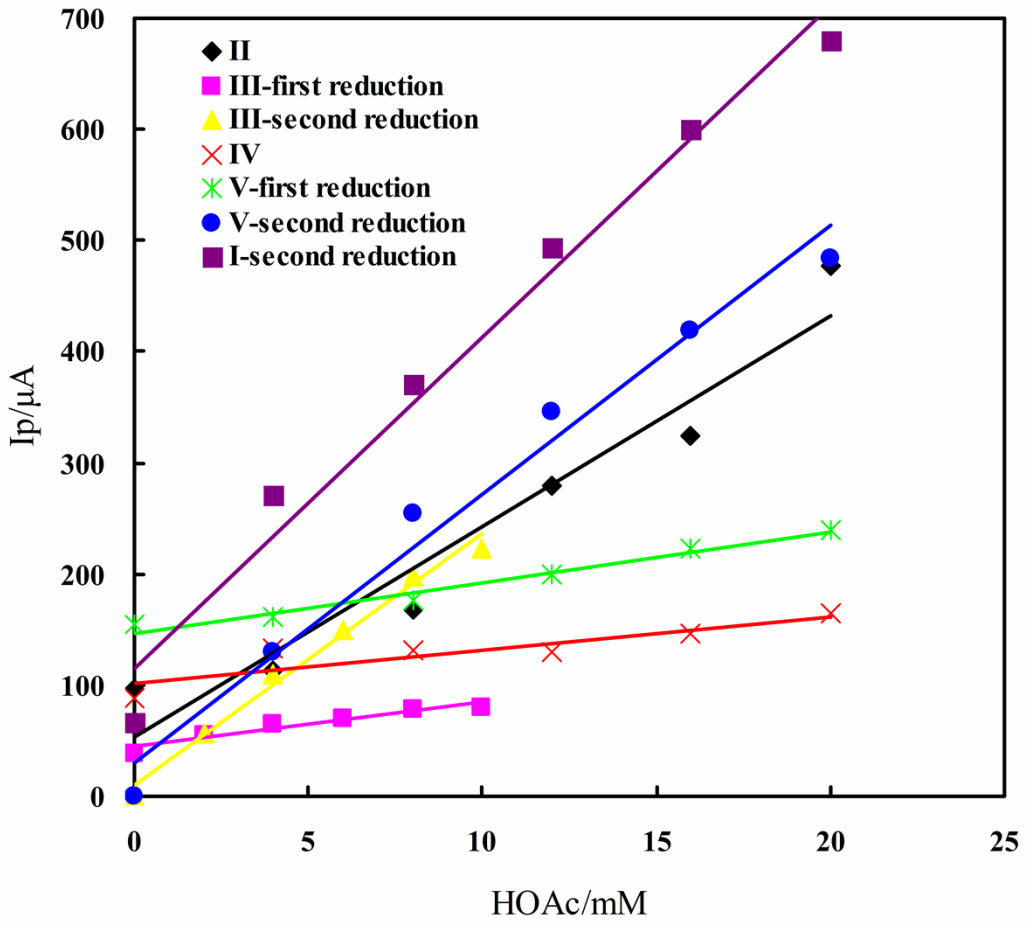

Figure S8. Dependence of current heights of electrocatalytic waves for the series of complexes (**I** (2 mM), **II** (2 mM), **III** (1 mM, Poor solubility), **IV** (2 mM) and **V** (2 mM)) on HOAc concentration (0, 2, 4, 6, 8, and 10 equiv.) in CH_3CN solution.

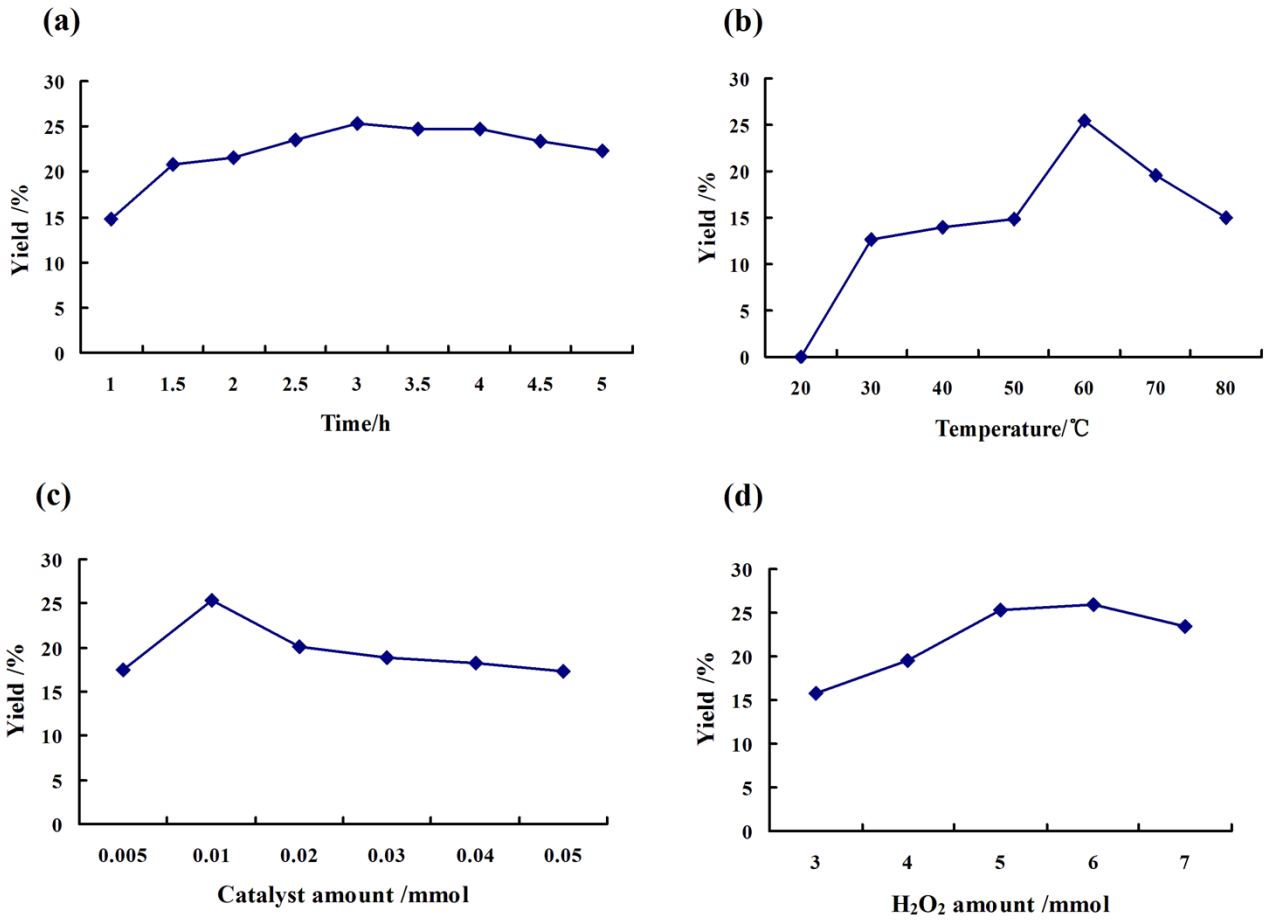

Figure S9. Effects of different parameters on hydroxylation of benzene to phenol.

a: **IV**, 0.01 mmol; benzene, 0.1 mL; CH_3CN, 2.0 mL; H_2O_2, 5.0 mmol; 60 °C.

b: **IV**, 0.01 mmol; benzene, 0.1 mL; CH_3CN, 2.0 mL; H_2O_2, 5.0 mmol; 3 h.

c: benzene, 0.1 mL; CH_3CN, 2.0 mL; H_2O_2, 5.0 mmol; 60 °C; 3 h.

d: **IV**, 0.01 mmol; benzene, 0.1 mL; CH_3CN, 2.0 mL; 60 °C; 3 h.

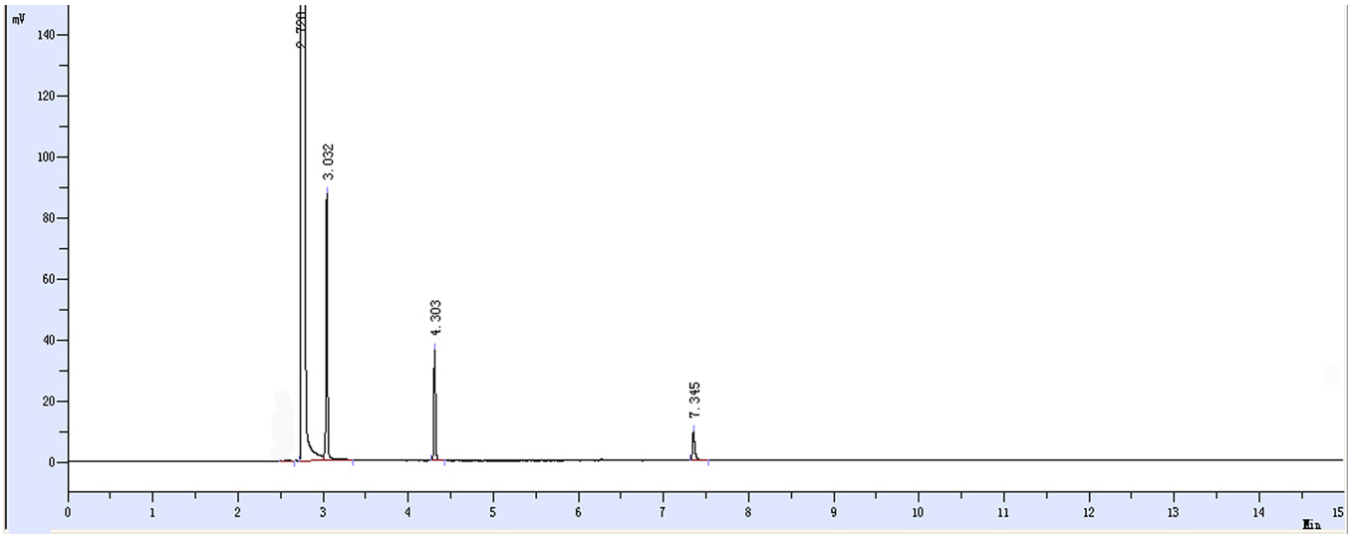

Figure S10. The GC of hydroxylation of benzene with H_2O_2 by **IV** under the optimized experimental conditions (**IV**, 0.01 mmol; benzene, 0.1 mL; CH_3CN, 2.0 mL; H_2O_2, 6.0 mmol; 60 °C; 3 h; yield 25.9%). No by-product was detected.

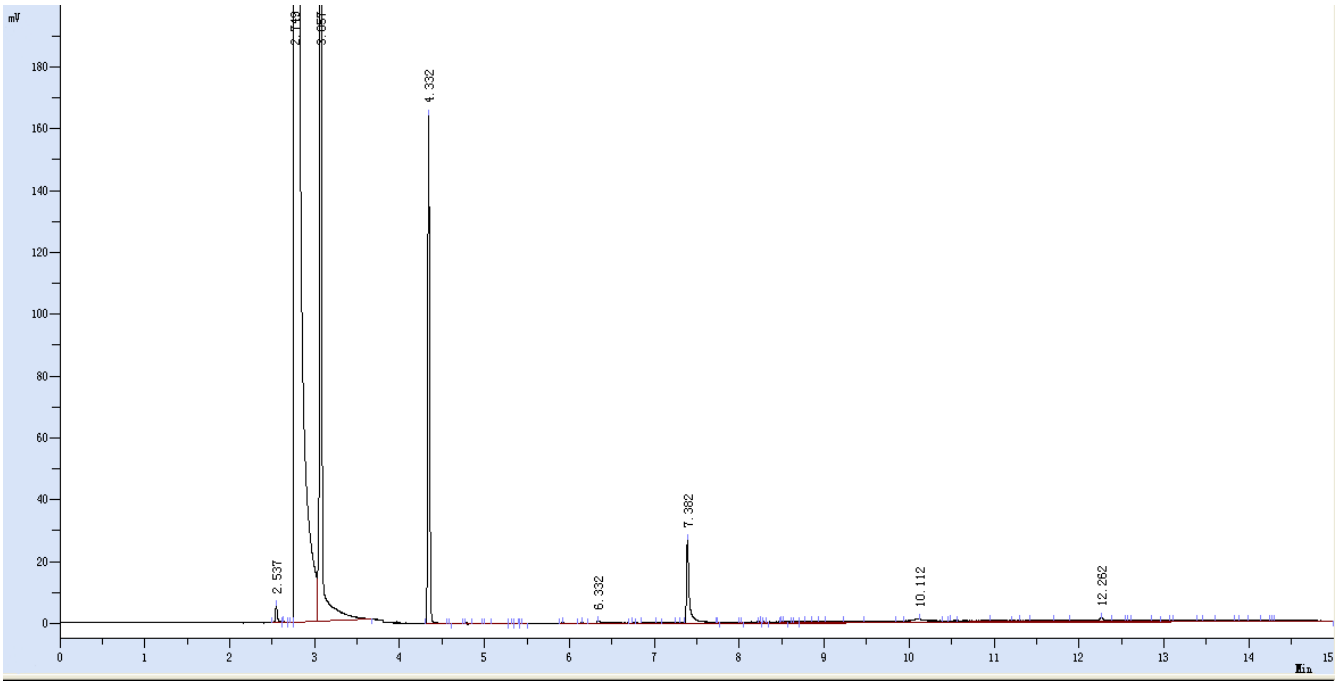

Figure S11. The GC of hydroxylation of benzene with H_2O_2 by **IV** under 70 °C (**IV**, 0.01 mmol; benzene, 0.1 mL; CH_3CN, 2.0 mL; H_2O_2, 6.0 mmol; 70 °C; 3 h). By-products were detected.

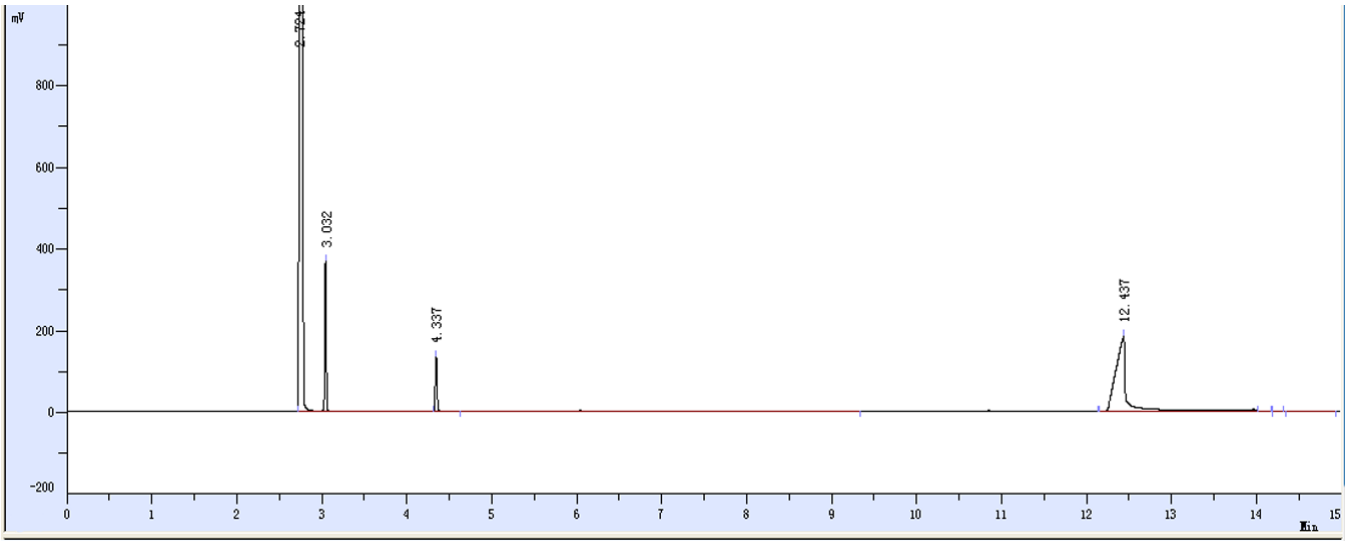

Figure S12. The GC of hydroxylation of benzene with *m*-CPBA by $FeSO_4$ under the experimental conditions ($FeSO_4$, 0.01 mmol; benzene, 0.1 mL; CH_3CN, 2.0 mL; *m*-CPBA, 6.0 mmol; 60 °C; 3 h). No phenol was detected.

Table S2. Retention times and the corresponding constituents of Figure S9 and Figure S10.

Retention time/min	2.7	3.0	4.3	7.3	12.4
Constituent	Acetonitrile	Benzene	Chlorobenzene	Phenol	*m*-Chlorobenzoic Acid